

Finite Scale Lyapunov Analysis of Temperature Fluctuations in Homogeneous Isotropic Turbulence

Nicola de Divitiis

"La Sapienza" University, Dipartimento di Ingegneria Meccanica e Aerospaziale, Via Eudossiana, 18, 00184 Rome, Italy

Abstract

This study analyzes the temperature fluctuations in incompressible homogeneous isotropic turbulence through the finite scale Lyapunov analysis of the relative motion between two fluid particles. The analysis provides an explanation of the mechanism of the thermal energy cascade, leads to the closure of the Corrsin equation, and describes the statistics of the longitudinal temperature derivative through the Lyapunov theory of the local deformation and the thermal energy equation. The results here obtained show that, in the case of self-similarity, the temperature spectrum exhibits the scaling laws κ^n , with $n \approx -5/3, -1$ and $-17/3 \div -11/3$ depending upon the flow regime. These results are in agreement with the theoretical arguments of Obukhov–Corrsin and Batchelor and with the numerical simulations and experiments known from the literature. The PDF of the longitudinal temperature derivative is found to be a non-gaussian distribution function with null skewness, whose intermittency rises with the Taylor scale Péclet number. This study applies also to any passive scalar which exhibits diffusivity.

Keywords: Lyapunov Analysis, Corrsin equation, von Kármán–Howarth equation, Self-Similarity

1. Introduction

This work adopts the finite-scale Lyapunov theory for studying the temperature fluctuations in incompressible homogeneous isotropic turbulence in an infinite fluid domain. The study is mainly motivated by the fact that, in isotropic turbulence, the temperature spectrum $\Theta(\kappa)$ exhibits several scaling laws κ^n in the different wavelength ranges depending on R and

Pr (Corrsin (JAP 1951); Obukhov (1949); Batchelor (1959); Batchelor et al (1959)), where R and Pr are Taylor scale Reynolds number and Prandtl number, respectively. This is due to the peculiar connection between temperature fluctuations, fluid deformation and velocity field, whose effect varies following R and Pr .

For large values of R and Pr , Corrsin (JAP 1951) and Obukhov (1949) argued, through the dimensional analysis, that $\Theta(\kappa) \approx \kappa^{-5/3}$ in the so-called inertial-convective subrange (see Fig. 1). Batchelor (1959) considered the isotropic turbulence at high Prandtl number, when R is assigned. There, the author assumed that, at distances less than the Kolmogorov scale, the temperature fluctuations are mainly related to the strain rate associated to the smallest scales of the velocity field. As the result, he showed that $\Theta \approx \kappa^{-1}$ in the so-called viscous-convective interval, a region where the scales are less than the Kolmogorov length (see Fig. 1). Different experiments dealing with the grid turbulence (Gibson & Schwarz (1963); Mydlarski & Warhaft (1998)) and calculations of the temperature spectrum through numerical simulations (see Donzis et al (2010) and references therein) confirm that $\Theta(\kappa)$ follows such these scaling laws.

On the contrary, when Pr is very small, the high fluid conductivity determines quite different situations with respect to the previous ones. Batchelor et al (1959) analyzed the small-scale variations of temperature fluctuations in the case of large conductivity, and found that $\Theta(\kappa) \approx \kappa^{-17/3}$, whereas Rogallo et al (1989) calculated the temperature spectra through numerical simulations of a passive scalar convected by a velocity field with zero correlation time. Rogallo et al (1989) showed that, when the kinetic energy spectrum follows the Kolmogorov law $E(\kappa) \approx \kappa^{-5/3}$, the temperature spectrum varies according to $\Theta(\kappa) \approx \kappa^n$, with $n \approx -11/3$.

According to the experiments of grid turbulence, temperature and velocity correlations are linked with each other when $Pr = O(1)$, whereas the decay rate and characteristic scales depend on the initial conditions. Specifically, Mills et al (1958) obtained very important data about the air turbulence behind a heated grid. They carried out several measurements of nearly isotropic fluctuations of velocity and temperature at different distances from the grid, and recognized that $f_\theta \simeq f$ and $p_* \simeq k$, where f_θ and f are temperature and velocity correlations respectively, p_* is the triple correlation temperature-velocity, and k is the longitudinal triple velocity correlation. Later, Warhaft & Lumley (1978) experimentally showed that spectrum shape and decay rate depend upon the initial conditions and that

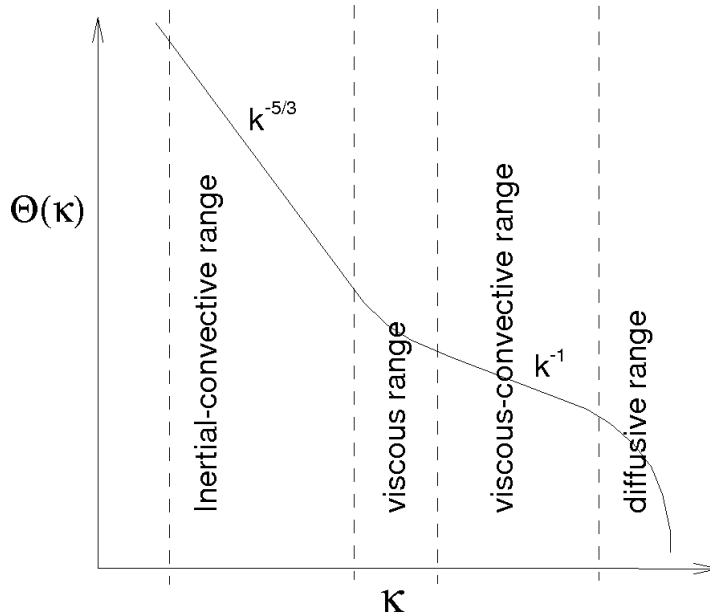


Figure 1: Scheme of the subranges of the temperature spectrum at high Prandtl numbers

the mechanical–thermal time scale ratio tends to a value close to the unity.

Other important characteristics of $\Theta(\kappa)$ is the self–similarity. This is related to the idea that the combined effect of thermal and kinetic energy cascade in conjunction with conductivity and viscosity, makes the temperature correlation similar in the time. This property was theoretically studied by George (see George (1988, 1992) and references therein) which showed that the decaying isotropic turbulence reaches the self–similarity, where $\Theta(\kappa)$ is scaled by the Taylor microscale whose current value depends on the initial condition. Recently, Antonia et al (2004) studied the temperature structure functions in decaying homogeneous isotropic turbulence and found that the standard deviation of the temperature, as well as the turbulent kinetic energy, follows approximately the similarity over a wide interval of length scales. There, the authors used this approximate similarity to calculate the third–order correlations and found satisfactory agreement between measured and calculated functions.

Very important advances, regarding other properties of passive scalars in fully developed turbulence, were recently made (Fereday & Haynes (2004); Schekochihin et al (2004); Doering & Thiffeault (2006); Tran (2007, 2008); Burton (2008)).

Fereday & Haynes (2004) studied the decay in a large-scale flow and discussed the relation between the decay obtained by the Lagrangian stretching theories and that calculated with the numerical simulations. Among the other things, the authors determined that the PDF of a passive scalar exhibits algebraic tails, with an exponent of about -3 in a given interval of dimensionless scalar concentration, with a cutoff due to the fluid diffusivity. For what concerns the decay models of a passive scalar, Schekochihin et al (2004) analyzed the case with single-scale random velocity field, and showed that, if there exists separation between flow scale and the box size, the decay rate is the result of the turbulent diffusion of the box-scale. Later, Doering & Thiffeault (2006) studied the mixing efficiency of a passive scalar subject to a steady and inhomogeneous source, advected by a statistically homogeneous and isotropic incompressible velocity field. The authors found that the mixing efficiency is limited by the values of Pr R and by specific characteristics of the source, and that the scaling laws of the bounds at high Pr R depend on the length scales of the source. Tran (2007), in an article dealing with the scalar diffusion in shear flows, determined an upper bound for the decay rate of the temperature standard deviation in the case of shear flows with bounded velocity gradients, where the initial temperature distribution is supposed to be a smooth function of the space co-ordinates. Thereafter, Tran (2008) analyzed the evolution of the temperature gradient and showed, thanks to the hypothesis of finite velocity gradient, that the square of temperature gradient and its decay rate are both bounded. Next, Burton (2008) extended the nonlinear large-eddy simulation method to conditions with moderate and very high Schmidt numbers, and, among the other things, provided the instantaneous field of scalar-energy at viscous-convective scales at high Schmidt-numbers.

From a theoretical point of view, the properties of $\Theta(\kappa)$ can be investigated through its evolution equation. $\Theta(\kappa)$ is the Fourier-Transform of f_θ which varies according to the Corrsin equation (Corrsin (JAS 1951)). This latter includes G , a term responsible for the thermal energy cascade that is directly related to the triple correlation p_* , thus the Corrsin equation is not closed. As G depends also on the velocity fluctuations, the Corrsin equation requires the knowledge of f , thus it must be solved together to the von Kármán-Howarth equation. On this argument, some work has been written. For instance, Baev & Chernykh (2010) (and references therein) studied temperature and kinetic energy spectra adopting a closure model based on the

gradient hypothesis, which incorporates empirical constants. Nevertheless, to the author’s knowledge, the estimation of $\Theta(\kappa)$ based on the theoretical analysis of the closure of von Kármán-Howarth and Corrsin equations has not received due attention.

This is the motivation of the present work, whose main objective is to propose the closure of the Corrsin equation and a description of the statistics of the temperature derivative. The present study is based on the finite-scale Lyapunov theory used by de Divitiis (2010, 2011). Here, this Lyapunov theory gives G in function of f and of $\partial f_\theta/\partial r$, and describes also the statistics of the temperature gradient through the analysis of the local strain and the canonical decomposition of temperature and velocity in terms of proper stochastic variables. The mathematical expression of G is obtained considering that it is frame invariant, thus G can be calculated in a convenient frame of reference. The adoption of the finite-scale Lyapunov basis is revealed to be a convenient choice for determining G . For what concerns the von Kármán-Howarth equation, the analytical closure proposed by de Divitiis (2010) is here used. Through the self-similarity, the closed von Kármán-Howarth and Corrsin equations are reduced to be an ordinary differential system. This latter is numerically solved for several values of R and Pr , and the obtained results show that the temperature spectrum exhibits scaling laws depending on R and Pr , in agreement with the experimental and theoretical data of the literature (Corrsin (JAP 1951); Obukhov (1949); Rogallo et al (1989); Mills et al (1958); Gibson & Schwarz (1963)). As far as the statistics of the longitudinal temperature gradient is concerned, it is represented by non-gaussian PDF with null skewness and a Kurtosis greater than three whose value rises with the Péclet number $Pe = Pr R$.

2. Background: Corrsin equation

For the sake of convenience, the procedure to obtain the Corrsin equation is here renewed.

Velocity and temperature are considered to be statistically homogeneous isotropic fields, and viscosity ν and thermal conductivity k are assigned quantities. The equations of the temperature fluctuation ϑ in two points $\mathbf{x} \equiv (x, y, z)$ and $\mathbf{x}' \equiv \mathbf{x} + \mathbf{r}$, are

$$\frac{\partial \vartheta}{\partial t} + \frac{\partial \vartheta}{\partial x_k} u_k - \chi \frac{\partial^2 \vartheta}{\partial x_k \partial x_k} = 0 \quad (1)$$

$$\frac{\partial \vartheta'}{\partial t} + \frac{\partial \vartheta'}{\partial x'_k} u'_k - \chi \frac{\partial^2 \vartheta'}{\partial x'_k \partial x'_k} = 0 \quad (2)$$

being $\mathbf{r} = (r_x, r_y, r_z)$ the separation vector, $\chi = k/(\rho C_p)$ is the fluid thermal diffusivity, and C_p is the specific heat at constant pressure. As well known, the evolution equation of the temperature correlation is determined multiplying Eq. (1) and (2) by ϑ' and ϑ , respectively, and summing the equations (Corrsin (JAS 1951)). The so obtained equation, averaged with respect to the ensemble of the temperature fluctuations, leads to

$$\theta^2 \frac{\partial f_\theta}{\partial t} + f_\theta \frac{d\theta^2}{dt} - G - 2\chi\theta^2 \left(\frac{\partial^2 f_\theta}{\partial r^2} + \frac{2}{r} \frac{\partial f_\theta}{\partial r} \right) = 0 \quad (3)$$

where

$$f_\theta = \frac{\langle \vartheta \vartheta' \rangle}{\theta^2} \quad (4)$$

is the temperature correlation function, $\theta = \sqrt{\langle \vartheta^2 \rangle}$ is the standard deviation of the temperature fluctuations, constant in the space, and

$$G = -\frac{\partial}{\partial r_k} \langle \vartheta \vartheta' (u'_k - u_k) \rangle \quad (5)$$

The first two terms of Eq. (3) express the time variations of f_θ and θ , whereas G , arising from the convective terms, provides the mechanism of the thermal energy cascade where $\partial \langle \cdot \rangle / \partial x'_k = -\partial \langle \cdot \rangle / \partial x_k = \partial \langle \cdot \rangle / \partial r_k$. The last term of Eq. (3) gives the effects of the thermal diffusion. Because of isotropy, $G(r)$ is an even function of $r \equiv |\mathbf{r}|$. According to Corrsin (JAS 1951,J), G is

$$G = 2 \left(\frac{\partial p_*}{\partial r} + 2 \frac{p_*}{r} \right) \equiv \frac{2}{r^2} \frac{\partial}{\partial r} (p_* r^2) \quad (6)$$

where $p_*(r)$ is the triple correlation between u_r and the temperatures in \mathbf{x} and \mathbf{x}' , i.e.

$$p_*(r) = \frac{\langle u_r \vartheta \vartheta' \rangle}{\theta^2 u} \quad (7)$$

and u_r is the longitudinal component of the fluid velocity. A property of $G(r)$ is that it does not modify θ , hence $G(0) = 0$ and $G \approx r^2$ near the origin.

Therefore, $p_* \approx r^3$ when $r \rightarrow 0$, and Eq. (3) gives the evolution equation for θ putting $r = 0$ (Corrsin (JAP 1951))

$$\frac{d\theta^2}{dt} = -12\chi \frac{\theta^2}{\lambda_\theta^2} \quad (8)$$

where λ_θ is the scale of the temperature correlation, or Corrsin microscale, defined as (Corrsin (JAS 1951))

$$\lambda_\theta = \sqrt{-\frac{2}{f_\theta''(0)}} \quad (9)$$

in which the superscript apex denotes the differentiation with respect to r . Hence, the evolution equation of f_θ is

$$\frac{\partial f_\theta}{\partial t} - 12\frac{\chi}{\lambda_\theta^2}f_\theta - G - 2\chi \left(\frac{\partial^2 f_\theta}{\partial r^2} + \frac{2}{r} \frac{\partial f_\theta}{\partial r} \right) = 0 \quad (10)$$

whose boundary conditions are

$$\begin{aligned} f_\theta(0) &= 1, \\ \lim_{r \rightarrow \infty} f_\theta(r) &= 0 \end{aligned} \quad (11)$$

Note that Eq. (10) depends also on the velocity fluctuations through $G(r)$ whose analytical form is not given at this stage of the analysis. Therefore, Eq. (10) is not closed and provides only a link between f_θ and G . Accordingly, the solutions f_θ of Eq. (10) will be related to f .

3. Lyapunov Analysis of thermal energy cascade: closure of Corrsin equation

This section analyses the thermal energy cascade using the finite-scale Lyapunov theory adopted in de Divitiis (2010), and proposes the analytical expression for G . For this purpose, consider now Eq. (5). As G is frame invariant, for the sake of convenience, it is expressed in the finite-scale Lyapunov basis E_λ . This basis is associated with the problem of the relative

motion between two fluid particles (de Divitiis (2010))

$$\begin{aligned}\frac{d\boldsymbol{\rho}}{dt} &= \mathbf{u}(\mathbf{x} + \boldsymbol{\rho}, t) - \mathbf{u}(\mathbf{x}, t), \\ \frac{d\mathbf{x}}{dt} &= \mathbf{u}(\mathbf{x}, t)\end{aligned}\tag{12}$$

where $\boldsymbol{\rho}$ gives the relative position between the particles, and \mathbf{u} varies according to the Navier–Stokes equations. To define E_λ , the solutions $\boldsymbol{\rho}_1$, $\boldsymbol{\rho}_2$ and $\boldsymbol{\rho}_3$ of Eq. (12) are first considered, whose initial conditions $\boldsymbol{\rho}_1(0)$, $\boldsymbol{\rho}_2(0)$ and $\boldsymbol{\rho}_3(0)$ correspond to mutually orthogonal vectors such that $|\boldsymbol{\rho}_1(0)| = |\boldsymbol{\rho}_2(0)| = |\boldsymbol{\rho}_3(0)|$. The basis E_λ is then obtained through the Gram-Schmidt orthonormalization process applied to $\boldsymbol{\rho}_1(t)$, $\boldsymbol{\rho}_2(t)$ and $\boldsymbol{\rho}_3(t)$.

In E_λ , the velocity difference fluctuation reads as (de Divitiis (2010))

$$\Delta\mathbf{u} \equiv \mathbf{u}' - \mathbf{u} = \lambda(r)\mathbf{r} + \boldsymbol{\omega}_\lambda \times \mathbf{r} + \boldsymbol{\zeta}\tag{13}$$

where λ is the maximal finite-scale Lyapunov exponent (associated with the length r), defined by $\lambda(r) \approx 1/T \int_0^T d\mathbf{r}/dt \cdot \mathbf{r}/r^2 dt$, and calculated in function of f as (de Divitiis (2010))

$$\lambda(r) = \frac{u}{r} \sqrt{2(1-f)}\tag{14}$$

$\boldsymbol{\omega}_\lambda$ is the angular velocity of E_λ with respect to the inertial frame of reference \mathfrak{R} , and $\boldsymbol{\zeta} \equiv (\zeta_1, \zeta_2, \zeta_3)$, related to the other two exponents, is expressed in E_λ as (de Divitiis (2010))

$$\zeta_1 = (\lambda_1 - \lambda)\varrho_1, \quad \zeta_2 = (\lambda_2 - \lambda)\varrho_2, \quad \zeta_3 = (\lambda_3 - \lambda)\varrho_3\tag{15}$$

where λ_1 , λ_2 and λ_3 are the Lyapunov exponents associated to the three directions ϱ_1 , ϱ_2 and ϱ_3 , respectively. Hence, λ is a deterministic quantity, whereas $\boldsymbol{\omega}_\lambda$ is a fluctuating variable related to the relative motion between E_λ and \mathfrak{R} . Without lack of generality, the coordinate ϱ_1 is supposed to be associated to the maximal exponent, then $\lambda_1 \rightarrow \lambda$, $\lambda_2 = \lambda_3 \equiv \lambda_\zeta$, ϱ_1 diverges being $|\varrho_1| \gg \gg |\varrho_2|, |\varrho_3|$, thus $\zeta_1 \rightarrow \hat{\zeta}_1 \neq 0$

$$\zeta_1 = \hat{\zeta}_1, \quad \zeta_2 = (\lambda_\zeta - \lambda)\varrho_2, \quad \zeta_3 = (\lambda_\zeta - \lambda)\varrho_3\tag{16}$$

The exponents $\lambda_2 = \lambda_3 \equiv \lambda_\zeta$ are determined by the continuity equation. With reference to Fig. 2, the equation is written considering, at a given time,

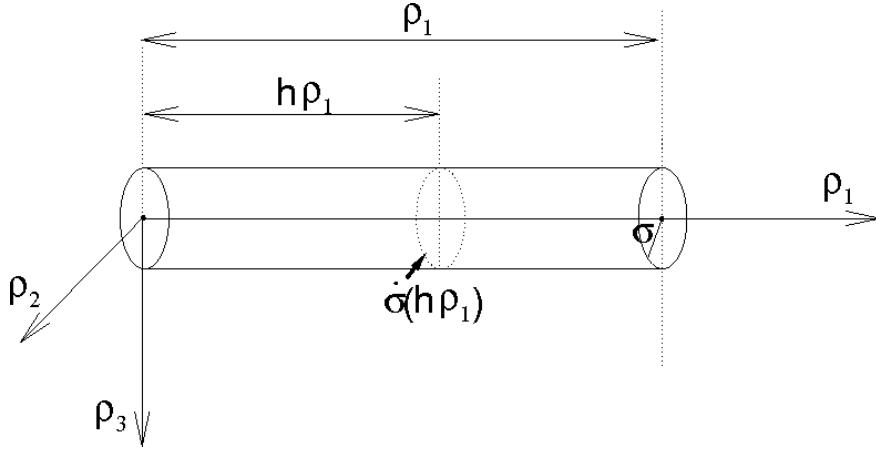


Figure 2: Scheme of Finite-scale Lyapunov basis embedded into a material cylinder, at a given time

the mass balance associated with a material circular cylinder whose axis is parallel to the direction ϱ_1

$$2\frac{\dot{\sigma}}{\sigma} + \frac{\dot{\varrho}_1}{\varrho_1} = 0 \quad (17)$$

where the dot denotes the differentiation with respect to t , $\dot{\sigma}$ is evaluated at the coordinate $h\varrho_1$, with $h \in (0, 1)$, whereas ϱ_1 and $\sigma \equiv \sqrt{\varrho_2^2 + \varrho_3^2}$ are the length and diameter of the cylinder. Therefore, $\dot{\varrho}_1/\varrho_1$ and $\dot{\sigma}/\sigma$ identify λ and λ_ζ , respectively, being

$$\lambda_\zeta = -\frac{\lambda}{2} \quad (18)$$

Substituting Eq. (13) into Eq. (5), and taking into account that λ is constant with respect to the operation of statistical average (i.e. $\langle \lambda \dots \rangle = \lambda \langle \dots \rangle$), G is the sum of three addends

$$G = G_1 + G_2 + G_3 \quad (19)$$

where

$$\begin{aligned}
G_1 &= -\frac{\partial}{\partial \varrho_k} (\langle \vartheta \vartheta' \rangle \lambda \varrho_k), \\
G_2 &= -\frac{\partial}{\partial \varrho_k} (\langle \vartheta \vartheta' \rangle \zeta_k), \\
G_3 &= -\frac{\partial}{\partial \varrho_k} (\varepsilon_{kij} \langle \vartheta \vartheta' \omega_i \rangle \varrho_j)
\end{aligned} \tag{20}$$

and ε_{kij} is the Levi–Civita tensor. The expression of G_1 is obtained taking into account the isotropy

$$G_1 = -\theta^2 \left(\frac{\partial f_\theta}{\partial r} \lambda r + \frac{f_\theta}{r^2} \frac{\partial}{\partial r} (r^3 \lambda) \right) \tag{21}$$

and G_2 is written considering that $\lambda(r)\mathbf{r} + \boldsymbol{\omega}_\lambda \times \mathbf{r} + \boldsymbol{\zeta}$ is solenoidal

$$G_2 = -\frac{\partial \langle \vartheta \vartheta' \rangle}{\partial \varrho_k} \zeta_k + \frac{f_\theta \theta^2}{r^2} \frac{\partial}{\partial r} (r^3 \lambda) \tag{22}$$

where $r^2 = \varrho_1^2 + \varrho_2^2 + \varrho_3^2$. For what concerns G_3 , it gives null contribution, as in isotropic turbulence, $\langle \vartheta \vartheta' \omega_i \rangle = L(|\boldsymbol{\rho}|) \varrho_i$, where $L(|\boldsymbol{\rho}|)$ is an even function of $|\boldsymbol{\rho}|$ (Batchelor (1953)). This implies that $G_3 \equiv 0$, thus G is

$$G = -\theta^2 \frac{\partial f_\theta}{\partial r} \lambda r - \frac{\partial \langle \vartheta \vartheta' \rangle}{\partial \varrho_k} \zeta_k \tag{23}$$

The first term of Eq. (23) is due to $\lambda > 0$ and provides in part the mechanism of the thermal energy cascade, whereas the second one, related to the other two Lyapunov exponents, exhibits the opposite sign. To obtain the second term, observe that into Eqs. (16), $\lambda_2 = \lambda_3 = \lambda_\zeta = -\lambda/2$, and this leads to

$$\frac{\partial \langle \vartheta \vartheta' \rangle}{\partial \varrho_2} \zeta_2 = \frac{3}{2} \frac{\partial f_\theta}{\partial r} \lambda \theta^2 \frac{\varrho_2^2}{r}, \quad \frac{\partial \langle \vartheta \vartheta' \rangle}{\partial \varrho_3} \zeta_3 = \frac{3}{2} \frac{\partial f_\theta}{\partial r} \lambda \theta^2 \frac{\varrho_3^2}{r} \tag{24}$$

Moreover, because of the isotropy $\partial \langle \vartheta \vartheta' \rangle / \partial \varrho_1 \hat{\zeta}_1$ must be of the form

$$\frac{\partial \langle \vartheta \vartheta' \rangle}{\partial \varrho_1} \hat{\zeta}_1 = \frac{3}{2} \frac{\partial f_\theta}{\partial r} \lambda \theta^2 \frac{\varrho_1^2}{r} \tag{25}$$

hence

$$\frac{\partial \langle \vartheta \vartheta' \rangle}{\partial r_k} \zeta_k = -\frac{3}{2} \theta^2 \frac{\partial f_\theta}{\partial r} \lambda r \quad (26)$$

Accordingly, the analytical expression of G is

$$G(r) = \frac{\theta^2}{2} \frac{\partial f_\theta}{\partial r} \lambda r = \theta^2 u \sqrt{\frac{1-f}{2}} \frac{\partial f_\theta}{\partial r} \quad (27)$$

Equation (27) gives the proposed closure of the Corrsin equation. Its main asset with respect to the other models is that it is not based on the phenomenological assumption, but is derived from a specific finite-scale Lyapunov analysis, under the assumption of incompressible homogeneous isotropic turbulence. Equation (27) preserves θ and describes the mechanism of the thermal energy cascade. This latter consists of a flow of the thermal energy from large to small scales whose effectiveness depends upon f and f_θ . According to the Lyapunov analysis of de Divitiis (2010), this mechanism can be viewed in the following manner. If, at an initial time t_0 , a toroidal material volume $\Sigma(t_0)$ is taken, which includes an assigned amount of thermal energy, its geometry and position change according to the fluid motion, and its dimensions will vary to preserve the volume. Choosing Σ in such a way that its maximal dimension R increases with t , the finite-scale Lyapunov analysis leads to $R \approx R(t_0) e^{\lambda(t-t_0)}$. That is, the thermal energy, initially enclosed into $\Sigma(t_0)$, at the end of the fluctuation is contained into $\Sigma(t)$ whose dimensions are changed with respect to the initial time t_0 . Therefore, the thermal energy is transferred from large to small scales, resulting enclosed in a more thin toroid.

4. Formulation of the problem

At this stage of the analysis, the problem for determining f and f_θ is formulated through the closed von Kármán–Howarth and Corrsin equations, which are here reported

$$\frac{\partial f}{\partial t} = \frac{K(r)}{u^2} + 2\nu \left(\frac{\partial^2 f}{\partial r^2} + \frac{4}{r} \frac{\partial f}{\partial r} \right) + \frac{10\nu}{\lambda_T^2} f \quad (28)$$

$$\frac{\partial f_\theta}{\partial t} = \frac{G(r)}{\theta^2} + 2\chi \left(\frac{\partial^2 f_\theta}{\partial r^2} + \frac{2}{r} \frac{\partial f_\theta}{\partial r} \right) + \frac{12\chi}{\lambda_\theta^2} f_\theta \quad (29)$$

where K and G are expressed by means of Eqs. (90) and (27)

$$\begin{aligned} K &= u^3 \sqrt{\frac{1-f}{2}} \frac{\partial f}{\partial r}, \\ G &= \theta^2 u \sqrt{\frac{1-f}{2}} \frac{\partial f_\theta}{\partial r} \end{aligned} \quad (30)$$

The boundary conditions of Eqs. (28) and (29) are

$$\begin{aligned} f(0) &= 1, & \lim_{r \rightarrow \infty} f(r) &= 0, \\ f_\theta(0) &= 1, & \lim_{r \rightarrow \infty} f_\theta(r) &= 0 \end{aligned} \quad (31)$$

As χ and ν are considered to be assigned quantities, according to Eqs. (28) and (29), the solutions f_θ are related to f , whereas f will not depend upon f_θ . The energy spectrum $E(\kappa)$ and the transfer function $T(\kappa)$ are the Fourier transforms of f and K (Batchelor (1953))

$$\begin{bmatrix} E(\kappa) \\ T(\kappa) \end{bmatrix} = \frac{1}{\pi} \int_0^\infty \begin{bmatrix} u^2 f(r) \\ K(r) \end{bmatrix} \kappa^2 r^2 \left(\frac{\sin \kappa r}{\kappa r} - \cos \kappa r \right) dr \quad (32)$$

as well as the temperature spectrum $\Theta(\kappa)$ and the temperature transfer function $\Gamma(\kappa)$ are calculated as (Ogura (1958))

$$\begin{bmatrix} \Theta(\kappa) \\ \Gamma(\kappa) \end{bmatrix} = \frac{2}{\pi} \int_0^\infty \begin{bmatrix} \theta^2 f_\theta(r) \\ G(r) \end{bmatrix} \kappa r \sin \kappa r dr \quad (33)$$

in such a way that

$$f_\theta(r) = \int_0^\infty \Theta(\kappa) \frac{\sin \kappa r}{\kappa r} d\kappa, \quad G(r) = \int_0^\infty \Gamma(\kappa) \frac{\sin \kappa r}{\kappa r} d\kappa \quad (34)$$

and

$$\int_0^\infty \Theta(\kappa) d\kappa = \theta^2, \quad \int_0^\infty \Gamma(\kappa) d\kappa = 0 \quad (35)$$

5. Lyapunov analysis of temperature fluctuations

This section presents the procedure for calculating the temperature fluctuations, which is based on the Lyapunov analysis of the fluid strain (de Divitiis (2010)), and on Eq. (1).

In order to obtain the temperature fluctuation, consider now the relative motion between two contiguous particles, expressed by the infinitesimal separation vector $d\mathbf{x}$ which obeys to the equation

$$d\dot{\mathbf{x}} = \nabla \mathbf{u} d\mathbf{x} \quad (36)$$

where the velocity gradient follows the Navier–Stokes equations. As observed by de Divitiis (2010), in turbulence, $d\mathbf{x}$ is much faster than the fluid state variables, and the Lyapunov analysis of Eq. (36) provides the local deformation in terms of maximal Lyapunov exponent $\Lambda \equiv \lambda(0) > 0$

$$\frac{\partial \mathbf{x}}{\partial \mathbf{x}_0} \approx e^{\Lambda(t-t_0)} \quad (37)$$

Now, the map $\chi : \mathbf{x}_0 \rightarrow \mathbf{x}$, is the function which determines the current position \mathbf{x} of a fluid particle located at the referential position \mathbf{x}_0 at $t = t_0$ (Truesdell (1977)). Equation (1) can be written in terms of the referential position \mathbf{x}_0

$$\frac{\partial \vartheta}{\partial t} = \left(-\frac{\partial \vartheta}{\partial x_{0p}} u_h + \chi \frac{\partial^2 \vartheta}{\partial x_{0p} \partial x_{0q}} \frac{\partial x_{0q}}{\partial x_h} \right) \frac{\partial x_{0p}}{\partial x_h} \quad (38)$$

The adoption of the referential coordinates allows to factorize the temperature fluctuation and to express it in the Lyapunov exponential form of the local deformation. As this deformation is assumed to be much more rapid than $\partial \vartheta / \partial x_{0p} u_h$ and $\chi \partial^2 \vartheta / \partial x_{0p} \partial x_{0q}$, the temperature fluctuation can be obtained integrating Eq. (38) with respect to the time, where $\partial \vartheta / \partial x_{0p} u_h$ and $\chi \partial^2 \vartheta / \partial x_{0p} \partial x_{0q}$ are considered to be constant

$$\vartheta \approx \frac{1}{\Lambda} \left(-\frac{\partial \vartheta}{\partial x_{0p}} u_h + \chi \frac{\partial^2 \vartheta}{\partial x_{0p} \partial x_{0q}} \right)_{t=t_0} \approx \frac{1}{\Lambda} \left(\frac{\partial \vartheta}{\partial t} \right)_{t=t_0} \quad (39)$$

This assumption is justified by the fact that, according to the classical formulation of motion of continuum media (Truesdell (1977)), $\partial \vartheta / \partial x_{0p} u_h$ and $\chi \partial^2 \vartheta / \partial x_{0p} \partial x_{0q}$ are smooth functions of t –at least during the period of a

fluctuation— whereas the fluid deformation varies very rapidly according to Eqs. (36)-(37).

For what concerns the temperature gradient, its evolution is described by an equation arising from Eq. (39)

$$\frac{\partial}{\partial t} \nabla \vartheta \approx \Lambda \nabla \vartheta \quad (40)$$

Although $\Lambda > 0$ determines the exponential growth of $\nabla \vartheta$, $\Lambda \approx \sqrt{\langle \|\nabla \mathbf{u}\|^2 \rangle}$ is a bounded quantity and this excludes that $\nabla \vartheta$ can diverge in finite time. This is in line with Tran (2008), where the temperature gradient is shown to be bounded due to the smoothness of $\nabla \mathbf{u}$.

6. Statistical analysis of temperature derivative

As explained in this section, the Lyapunov analysis of the local deformation and some plausible assumptions about the statistics of \mathbf{u} and ϑ lead to the calculation of the distribution function of $\partial \vartheta / \partial r$ and of all its dimensionless statistical moments.

The statistical properties of $\partial \vartheta / \partial r$, are here investigated expressing velocity and temperature through the following canonical decomposition (Ventsel (1973); de Divitiis (2013))

$$\mathbf{u} = \sum_k \hat{\mathbf{U}}_k \xi_k, \quad \vartheta = \sum_k \hat{\Theta}_k \xi_k \quad (41)$$

where $\hat{\mathbf{U}}_k$ and $\hat{\Theta}_k$ are proper coordinate functions of t and \mathbf{x} , and ξ_k ($k = 1, 2, \dots$) are dimensionless independent stochastic variables which satisfy

$$\langle \xi_k \rangle = 0, \quad \langle \xi_i \xi_j \rangle = \delta_{ij}, \quad \langle \xi_i \xi_j \xi_k \rangle = \varpi_{ijk} p, \quad |p| \gg \gg 1, \quad \langle \xi_k^4 \rangle = O(1) \quad (42)$$

where $\varpi_{ijk} = 1$ for $i = j = k$, else $\varpi_{ijk} = 0$. According to de Divitiis (2013), the variables ξ_k are chosen in such a way that $|\langle \xi_k^3 \rangle| \gg \gg 1$, $k = 1, 2, \dots$ so that ξ_k can describe the mechanism of thermal and kinetic energy cascade.

The dimensionless temperature fluctuation $\hat{\vartheta}$ is obtained in terms of ξ_k substituting Eq. (41) into Eq. (39)

$$\hat{\vartheta} = \sum_{ij} A_{ij} \xi_i \xi_j + \frac{1}{Pe} \sum_k b_k \xi_k \quad (43)$$

where $r = \hat{r}\lambda_T$, $\vartheta = \hat{\vartheta} \theta$, whereas $Pe = R Pr$ and $R = u\lambda_T/\nu$ are Péclet and Reynolds numbers referred to the Taylor scale, and $Pr = \nu/\chi$ is the fluid Prandtl number, therefore $\sum_{ij} A_{ij}\xi_i\xi_j$ and $1/Pe \sum_k b_k\xi_k$ arise from convective term and fluid conduction, respectively. Thanks to the isotropy, both \mathbf{u} and ϑ are two gaussian stochastic variables (Ventsel (1973); Lehmann (1999)), accordingly, Eq. (43) satisfies the Lindeberg condition, a very general necessary and sufficient condition for satisfying the central limit theorem (Ventsel (1973); Lehmann (1999)). This condition does not apply to $\partial\vartheta/\partial r \equiv \lim_{r \rightarrow 0} \Delta\vartheta/r$. In fact, as $\Delta\vartheta$ is the difference between two correlated gaussian variables, its PDF could be a non-gaussian distribution function.

Now, to obtain the PDF of the dimensionless temperature gradient, the fluctuation $\partial\hat{\vartheta}/\partial\hat{r}$ is first calculated in function of ξ_k

$$\frac{\partial\hat{\vartheta}}{\partial\hat{r}} = \sum_{ij} \frac{\partial A_{ij}}{\partial\hat{r}} \xi_i \xi_j + \frac{1}{Pe} \sum_k \frac{\partial b_k}{\partial\hat{r}} \xi_k \equiv L + S + P + N \quad (44)$$

This fluctuation consists of the contributions L , S , P and N , appearing into Eq. (44): in particular, L is the sum of all linear terms due to the fluid conductivity, $S \equiv S_{ij}\xi_i\xi_j$ is the sum of all semidefinite bilinear forms arising from the convective term, whereas P and N are, respectively, the sums of definite positive and negative quadratic forms, which derive from the convective term. The quantity $L + S$ tends to a gaussian random variable being the sum of statistically orthogonal terms, while P and N do not, as they are linear combinations of squares (Madow (1940); Lehmann (1999)). Their general expressions are $P = P_0 + \eta_1 + \eta_2^2$, $N = N_0 + \zeta_1 - \zeta_2^2$, where P_0 and N_0 are constants, and η_1 , η_2 , ζ_1 and ζ_2 are four different centered random gaussian variables which are mutually uncorrelated thanks to the hypotheses of fully developed chaos and isotropy. Therefore, the longitudinal fluctuation of the temperature derivative can be written as

$$\frac{\partial\hat{\vartheta}}{\partial\hat{r}} = \psi_1\xi + (\psi_2(\eta^2 - 1) - \psi_3(\zeta^2 - 1)) \quad (45)$$

where ξ , η and ζ are independent gaussian centered random variables for which $\langle \xi^2 \rangle = \langle \eta^2 \rangle = \langle \zeta^2 \rangle = 1$, and ψ_1 , ψ_2 and ψ_3 are given quantities. Due to the isotropy, the skewness of $\partial\hat{\vartheta}/\partial r$ must be equal to zero, thus $\psi_2 = \psi_3$, and

$$\frac{\partial\hat{\vartheta}}{\partial\hat{r}} = \psi_1\xi + \psi_2(\eta^2 - \zeta^2) \quad (46)$$

Furthermore, comparing the terms of Eqs. (46) and (44), we obtain that ψ_1 and ψ_2 are related with each other and that their ratio $\psi = \psi_1/\psi_2$ depends on the Péclet number

$$\frac{4\psi_2^2}{\psi_1^2} = \frac{\langle (P + N)^2 \rangle}{\langle (S_{ij}\xi_i\xi_j + 1/Pe \partial b_k/\partial \hat{r}\xi_k)^2 \rangle} \quad (47)$$

Taking into account the properties (42) of ξ_k ($\langle \xi_k^3 \rangle \gg 1$, $\langle \xi_k^4 \rangle = O(1)$), and in view of Eq. (47), we found

$$\psi \equiv \frac{\psi_2}{\psi_1} = C\sqrt{Pe} \quad (48)$$

where C is a proper constant which has to be identified. Hence, the dimensionless longitudinal temperature derivative is

$$\frac{\vartheta_r}{\sqrt{\langle \vartheta_r^2 \rangle}} = \frac{\xi + \psi(\eta^2 - \zeta^2)}{\sqrt{1 + 4\psi^2}} \quad (49)$$

In order to identify C , observe that Eq. (49) is formally similar to the expression of the longitudinal velocity derivative $\partial u_r/\partial r$ obtained in de Divitiis (2010) (see also the appendix)

$$\frac{\partial u_r/\partial r}{\sqrt{\langle (\partial u_r/\partial r)^2 \rangle}} = \frac{\xi_u + \psi_u(\chi(\eta_u^2 - 1) - (\zeta_u^2 - 1))}{\sqrt{1 + 2\psi_u^2(1 + \chi^2)}} \quad (50)$$

ξ_u , η_u and ζ_u are independent centered gaussian random variables with $\langle \xi_u^2 \rangle = \langle \eta_u^2 \rangle = \langle \zeta_u^2 \rangle = 1$, and

$$\psi_u(R) = \sqrt{\frac{R}{15\sqrt{15}}} \hat{\psi}_u(0), \quad \hat{\psi}_u(0) = O(1), \quad \chi = \chi(R) = O(1) \quad (51)$$

$\chi \neq 1$ provides a negative skewness of $\partial u_r/\partial r$, whereas $\hat{\psi}_u(0) \simeq 1.075$ is determined through an approximate estimation of the critical value of R (de Divitiis (2010)). Now, when $Pr = 1$, it is reasonable to assume that the ratio between linear and quadratic terms of Eq. (49) is equal to that of the corresponding terms of Eq. (50). Accordingly, $\psi \simeq \psi_u$ and this identifies an approximate value of C

$$C \approx \frac{\hat{\psi}_u(0)}{15^{3/4}} \simeq 0.141 \quad (52)$$

The distribution function of the temperature derivatives is thus expressed through the Frobenius–Perron equation

$$F(\vartheta'_r) = \int_{\xi} \int_{\eta} \int_{\zeta} p(\xi)p(\eta)p(\zeta) \delta(\vartheta'_r - \vartheta_r(\xi, \eta, \zeta)) d\xi d\eta d\zeta \quad (53)$$

where $\vartheta_r(\xi, \eta, \zeta)$ is determined by Eq. (49), δ is the Dirac delta and p is a centered gaussian PDF with standard deviation equal to one.

Finally, the dimensionless statistical moments of ϑ_r are easily calculated considering that ξ , η and ζ are independent gaussian variables

$$H_n \equiv \frac{\langle \vartheta_r^n \rangle}{\langle \vartheta_r^2 \rangle^{n/2}} = \frac{1}{(1 + 4\psi^2)^{n/2}} \sum_{k=0}^n \binom{n}{k} \psi^k \langle \xi^{n-k} \rangle \langle (\eta^2 - \zeta^2)^k \rangle \quad (54)$$

It is worth remarking that, for non–isotropic turbulence or in more complex cases with boundary conditions, the stochastic variables ξ_k could not satisfy the Lindeberg condition, thus ϑ will be not distributed following a Gaussian PDF, and Eq. (49) changes its analytical form and can incorporate more intermittent terms (Lehmann (1999)) which give the deviation with respect to the isotropic turbulence. Hence, the absolute statistical moments of ϑ_r will be greater than those calculated with Eq.(54), indicating that, in a more complex situation than the isotropic turbulence, the intermittency of ϑ_r can be significantly stronger.

7. Self–Similar temperature spectrum

An ordinary differential equation which describes the spatial evolution of f_{θ} is now derived from Eq. (29), adopting the hypothesis of self–similarity of von Kármán & Lin (1949), George (1988, 1992), and using the proposed closure of the Corrsin equation.

The idea of self–preserving correlation function consists in what follows: far from the initial condition, the simultaneous effect of thermal and kinetic energy cascade with the fluid conductivity and viscosity acts keeping f_{θ} similar in the time. According to George (1988, 1992), f_{θ} can be scaled with respect to $\lambda_T(t)$, thus

$$f_{\theta} = f_{\theta}(\hat{r}), \text{ where } \hat{r} = \frac{r}{\lambda_T(t)} \quad (55)$$

Substituting Eq. (55) into Eq. (29), we obtain

$$-\frac{df_\theta}{d\hat{r}} \frac{\hat{r}}{u} \frac{d\lambda_T}{dt} = \sqrt{\frac{1-f}{2}} \frac{df_\theta}{d\hat{r}} + \frac{2}{R Pr} \left(\frac{d^2 f_\theta}{d\hat{r}^2} + \frac{2}{\hat{r}} \frac{df_\theta}{d\hat{r}} \right) + \frac{12}{R Pr} \left(\frac{\lambda_T}{\lambda_\theta} \right)^2 f_\theta \quad (56)$$

Therefore, the boundary problem given by Eqs. (29) and (31) is here reduced to an ordinary differential equation of the second order in the variable r . Equation (56) is a non-linear equation, and

$$\frac{du^2}{dt} = -\frac{10\nu u^2}{\lambda_T^2}, \quad \frac{d\theta^2}{dt} = -\frac{12k\theta^2}{\lambda_\theta^2} \quad (57)$$

describe the evolution of kinetic and thermal energies. Now, due to self-similarity, all the coefficients of Eq. (56) do not vary with the time (von Kármán & Howarth (1938); von Kármán & Lin (1949), George (1988, 1992)), thus

$$R = \text{const}, \quad \frac{1}{u} \frac{d\lambda_T}{dt} = \text{const}, \quad \frac{\lambda_\theta}{\lambda_T} = \text{const} \quad (58)$$

As λ_T follows Eq. (94) (see appendix), λ_θ is obtained from the constancy of λ_θ/λ_T

$$\lambda_\theta(t) = \lambda_\theta(0) \sqrt{1 + 10\nu t/\lambda_T^2(0)}. \quad (59)$$

Thus, according to Warhaft & Lumley (1978) and George (1988, 1992), the microscales λ_T , λ_θ and the rates $d\theta^2/dt$ and du^2/dt depend on the initial conditions of temperature and kinetic energy spectra. Taking into account Eq. (94), we obtain

$$\frac{1}{u} \frac{d\lambda_T}{dt} = \frac{5}{R} \quad (60)$$

The self-similar solutions are searched over the whole range of \hat{r} , but for the dimensionless distances whose order magnitude exceeds R . This corresponds to assume the self-similarity for all the frequencies of the energy spectrum, with the exception of the lowest ones (von Kármán & Howarth (1938); von Kármán & Lin (1949)). Accordingly, $\partial f_\theta/\partial t$ can be neglected with respect to the other terms, thus $f_\theta(\hat{r})$ obeys to the following non-linear ordinary differential equation

$$R Pr \sqrt{\frac{1-f}{2}} \frac{df_\theta}{d\hat{r}} + 2 \left(\frac{d^2 f_\theta}{d\hat{r}^2} + \frac{2}{\hat{r}} \frac{df_\theta}{d\hat{r}} \right) + 12 \left(\frac{\lambda_T}{\lambda_\theta} \right)^2 f_\theta = 0 \quad (61)$$

For $\hat{r} = 0$, Eq. (61) gives

$$\frac{d^2 f_\theta(0)}{d\hat{r}^2} = -2 \left(\frac{\lambda_T}{\lambda_\theta} \right)^2 \quad (62)$$

Hence, to calculate f_θ , λ_T/λ_θ must be first specified into Eq. (61). This is determined substituting Eq. (59) into Eq. (57) and integrating this latter from $t = 0$ to t

$$\ln \left(\frac{\theta(t)}{\theta(0)} \right) = -\frac{3}{5} \left(\frac{\lambda_T}{\lambda_\theta} \right)^2 \frac{1}{Pr} \ln \left(1 + \frac{10\nu}{\lambda_T(0)^2} t \right), \quad (63)$$

$$\ln \left(\frac{u(t)}{u(0)} \right) = -\frac{1}{2} \ln \left(1 + \frac{10\nu}{\lambda_T(0)^2} t \right)$$

The fully self-similarity (mechanical and thermal) occurs when θ and u are proportional to each other (George (1988, 1992))

$$\frac{\theta(t)}{\theta(0)} = \frac{u(t)}{u(0)} \quad (64)$$

Hence, the ratio λ_T/λ_θ satisfying this condition depends on the Prandtl's number

$$\frac{\lambda_\theta}{\lambda_T} = \sqrt{\frac{6}{5} \frac{1}{Pr}} \quad (65)$$

Accordingly, $f_\theta''(0)$ is related to Pr

$$\frac{d^2 f_\theta}{d\hat{r}^2}(0) = -\frac{5}{3} Pr \quad (66)$$

This self-similarity expresses a further link between f and f_θ .

Observe that the solutions $f_\theta \in C^2[0, \infty)$ of Eq. (61) with $df_\theta/d\hat{r}(0) = 0$ and $Pr \neq 0$, tend to zero as $r \rightarrow \infty$, thus the boundary condition (11) can be replaced by the following conditions in the origin

$$f_\theta(0) = 1, \quad \frac{df_\theta}{d\hat{r}}(0) = 0 \quad (67)$$

Therefore, the boundary problem represented by Eqs. (61) and (11), is reduced to the following initial condition problem written in the Cauchy's normal form

$$\begin{aligned}\frac{df_\theta}{d\hat{r}} &= F_\theta \\ \frac{dF_\theta}{d\hat{r}} &= -5 Pr f_\theta - \left(\frac{R Pr}{2} \sqrt{\frac{1-f}{2}} + \frac{2}{\hat{r}} \right) F_\theta\end{aligned}\tag{68}$$

the initial condition of which is

$$f_\theta(0) = 1, \quad F_\theta(0) = 0\tag{69}$$

In conclusion, the self-similar functions f and f_θ are calculated as the solutions of the ordinary differential system (96) and (68) with the initial conditions (97) and (69).

8. Results and Discussion

Temperature and velocity correlations are first calculated with Eqs. (96) and (68), for several values of R and Pr . Thereafter, the statistical analysis of $\partial\vartheta/\partial r$ is carried out using the Lyapunov theory of the temperature derivative.

The case with $Pr \rightarrow 0$ is first considered. This is a limit case of Eqs. (68)–(69) corresponding to the following equation

$$\frac{d^2 f_\theta}{d\hat{r}^2} + \frac{2}{\hat{r}} \frac{df_\theta}{d\hat{r}} = 0\tag{70}$$

which does not admit analytical solutions with the boundary conditions (31).

Conversely, when $Pr \rightarrow \infty$ ($\nu \gg \chi$),

$$\lim_{\hat{r} \rightarrow 0} \frac{d^2 f_\theta}{d\hat{r}^2} = -\infty\tag{71}$$

and this gives the behavior of f_θ near the origin. For $\hat{r} > 0$, f_θ is obtained solving Eqs. (68)–(69) by quadrature, in terms of f

$$\ln f_\theta(\hat{r}) = -\frac{10\sqrt{2}}{R} \int_0^{\hat{r}} \frac{d\xi}{\sqrt{1-f(\xi)}}\tag{72}$$

This equation implies that, if R is large enough and

$$f \simeq 1 - \left(\frac{r}{L_u}\right)^{2/3}, \quad \text{then also } f_\theta \simeq 1 - \left(\frac{r}{L_\theta}\right)^{2/3} \quad (73)$$

where $L_\theta = L_u$ are length scales proportional to λ_T

$$L_u = L_\theta = \frac{R}{15\sqrt{2}}\lambda_T, \quad (74)$$

Therefore, if $Pr \rightarrow \infty$, the ratios between the scales are

$$\frac{L_\theta}{L_u} = 1, \quad \frac{\lambda_\theta}{\lambda_T} = 0 \quad (75)$$

When R and Pr change, the ratios between the scales vary depending on the combined values of R and Pr , therefore quite different situations occur.

In order to study the influence of R and Pr on f_θ , Eqs. (96) and (68) are numerically solved for different values of R and Pr . The Reynolds number is assumed to be $R = 50, 100$ and 300 , whereas Pr ranges from 0.001 , to 10 . Figure 3 shows f (dashed line) and f_θ (solid lines). The temperature correlation, related to f through Eq. (27), is furthermore linked to f by self-similarity (see Eq. (65)). Therefore, when R and λ_T are given, the Corrsin microscale decreases as Pr rises, and the curves of f_θ seem to collapse into a single diagram when $Pr \rightarrow \infty$. On the contrary, small values of Pr determine large length scales of f_θ and p_* . The case with $R = 50$ is first considered. For $Pr = 0.001$, f_θ exhibits oscillations whose amplitude decreases as \hat{r} rises. When Pr increases, oscillations magnitude and Corrsin microscale diminish, and for $0.01 < Pr < 0.1$ such oscillations vanish, being $f_\theta > 0$. The case $R = 100$ differs from the previous one. The higher value of R determines a sizable reduction of the oscillations, whereas the dimensionless scales of f and f_θ are greater than the previous ones. Next, for $R = 300$, the dimensionless scales increase further, and $f_\theta > 0$ is a monotonic function of r for each value of Pr .

Accordingly, the triple correlation p_* varies with R and Pr . For $R = 50$, small values of Pr (0.001) correspond to large dimensionless scales and sizable oscillations of p_* , whereas higher Prandtl numbers give reductions of these oscillations and of the length scales. Increasing R ($R = 100$ and 300), the length scales rise, the oscillations disappear, and a reduction of $|p_*|_{MAX}$ is observed. When $Pr = 0.7$ and 1 , $f_\theta \approx f$, and $p_* \approx k$, and this is in very good

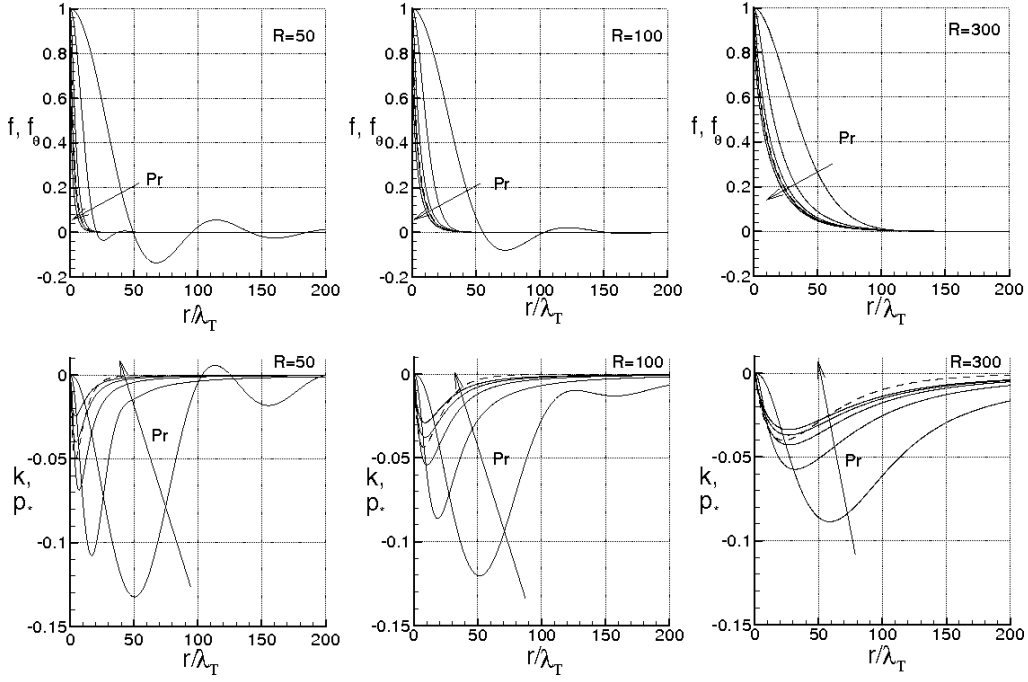


Figure 3: Correlation functions for $Pr= 10^{-3}, 10^{-2}, 0.1, 1.0$ and 10 , at different Reynolds numbers. Top: velocity correlation f (dashed line) and temperature correlation f_θ (solid lines). Bottom: triple velocity correlation k (dashed line) and triple velocity-temperature correlation p_* (solid lines)

agreement with the classical experiments of Mills et al (1958) which regards the turbulence behind heated grid.

As far as $f(r)$ and $k(r)$ are concerned, these agree with the results of de Divitiis (2011).

The temperature spectra $\Theta(\kappa)$, calculated with Eq. (32) and (33), are depicted in Fig. 4. The variations of $\Theta(\kappa)$ with R and Pr are quite peculiar and are consistent with the prior studies of the literature in the sense that there are regions where $\Theta(\kappa)$ exhibits different scaling laws $\Theta(\kappa) \approx \kappa^n$. In any case, according to Eq. (27), $n \rightarrow 2$, as $\kappa \rightarrow 0$. For $Pr = 0.001$, when R ranges from 50 to 300, the temperature spectrum shows essentially two regions (see also Fig. 5): one near the origin where $n \simeq 2$, and the other one, at higher values of κ , where $-17/3 < n < -11/3$, (value very close to $-13/3$). The exponent n varies rapidly at low Reynolds numbers, whereas for higher R , n exhibits more gradual variations. The value of $n \approx -13/3$, here obtained in an interval around to $\hat{r} \approx 1$, is in between the exponent proposed

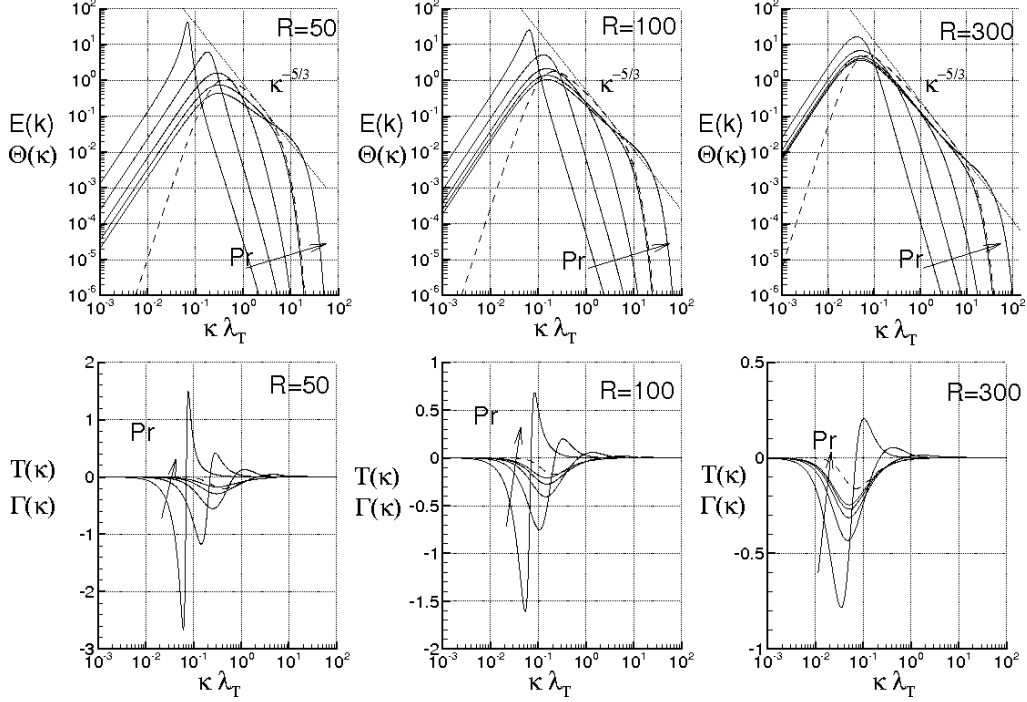


Figure 4: Spectra for $Pr = 10^{-3}, 10^{-2}, 0.1, 1.0$ and 10 , at different Reynolds numbers. Top: kinetic energy spectrum $E(\kappa)$ (dashed line) and temperature spectrum $\Theta(\kappa)$ (solid lines). Bottom: velocity transfer function $T(\kappa)$ (dashed line) and temperature transfer function $\Gamma(\kappa)$ (solid line)

by Batchelor et al (1959) ($-17/3$) and the value determined by Rogallo et al (1989) ($-11/3$) with the numerical simulations. Increasing κ , n strongly diminishes, and $\Theta(\kappa)$ does not show scaling law. With reference to Fig. 5, when $Pr=0.01$, the three curves intersect with each other for $0.1 < \hat{r} < 1$, where $n \simeq -5/3$ and the curves exhibit inflection points. Now, there is an interval near $\hat{r} \approx 1$ where $-17/3 < n < -13/3$, and this is in agreement with Batchelor et al (1959). For $Pr = 0.1$, the previous scaling law vanishes, whereas for $R = 50$ and 100 , n changes with κ , and $\Theta(\kappa)$ does not show clear scaling laws. When $R = 300$, the birth of a small region is observed, where $n \approx -5/3$ has an inflection point. For $Pr = 0.7$ and 1 , with $R = 300$, the width of this region is increased, whereas at $Pr = 10$, and $R = 300$, we observe two regions: one interval where n has a local minimum with $n \simeq -5/3$, and the other one where n exhibits a relative maximum, with $n \simeq -1$. For larger κ , n diminishes and the scaling laws disappear.

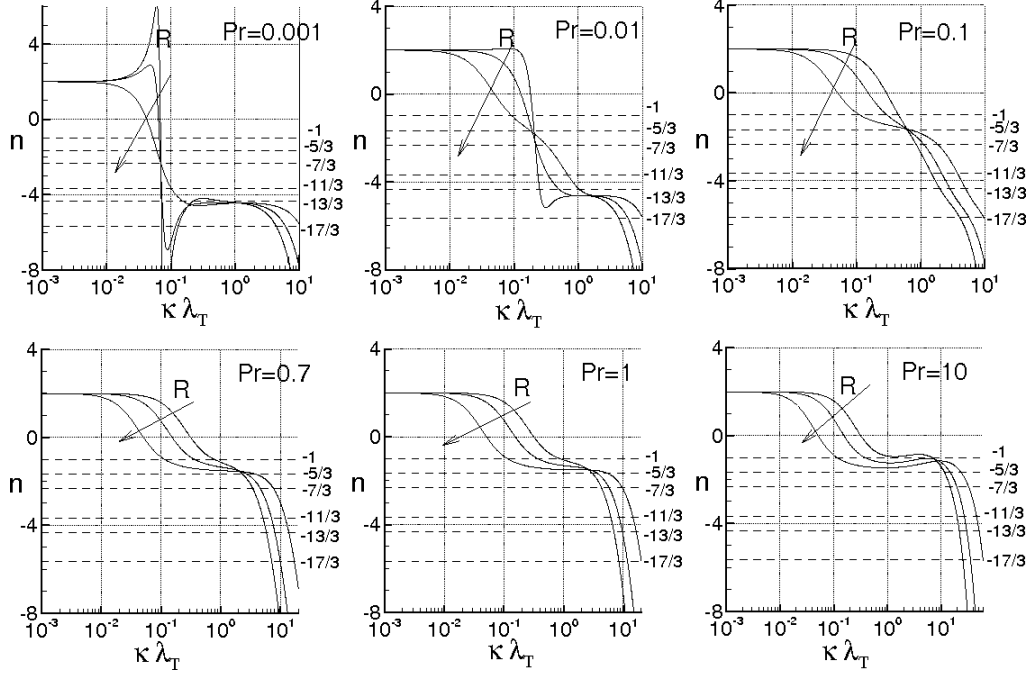


Figure 5: Scaling exponent of the temperature spectrum calculated for $Re = 50, 100$ and 300 , at different values of the Prandtl's number.

Figure 4 reports also (on the bottom) the spectra $\Gamma(\kappa)$ (solid lines) and $T(\kappa)$ (dashed lines) which describe the mechanism of kinetic and thermal energy cascade. As these latter do not modify the value of θ and u , $\int_0^\infty T(\kappa)d\kappa \equiv 0$, and $\int_0^\infty \Gamma(\kappa)d\kappa \equiv 0$.

The presence of the scaling law $n \simeq -5/3$ agrees with the theoretical arguments of Corrsin (JAP 1951); Obukhov (1949) (see also Mydlarski & Warhaft (1998); Donzis et al (2010) and references therein). For large values of R and Pr , $\Theta(\kappa)$ behaves like

$$\Theta(\kappa) = C_\theta \epsilon^{-1/3} \epsilon_\theta \kappa^{-5/3}, \quad (76)$$

in the inertial-convective range, where

$$\epsilon_\theta = 12\chi \frac{\theta^2}{\lambda_\theta^2}, \quad \epsilon = 15\nu \frac{u^2}{\lambda_T^2} \quad (77)$$

and C_θ is the so-called Corrsin-Obukhov constant, a quantity of the order of the unity. This study identifies C_θ by means of the obtained results. First,

the following quantity

$$F_C(\kappa) = \Theta(\kappa)\epsilon^{1/3}\kappa^{5/3}\epsilon_\theta^{-1} \quad (78)$$

–here called Corrsin function– is calculated in terms of κ , Re and Pr . Thereafter, C_θ is determined in such a way that $C_\theta = F_C(\kappa)$ in the range where $F_C(\kappa)$ is about constant. A different definition of the Corrsin–Obukhov constant $C_{\theta 1}$ can be made with respect to the one dimensional spectrum

$$\frac{d\Theta_1}{d\kappa_1}(\kappa_1) = -\frac{\Theta(\kappa_1)}{2\kappa_1}, \text{ where } \Theta_1(\kappa) = C_{\theta 1}\epsilon^{-1/3}\epsilon_\theta\kappa^{-5/3} \text{ and } C_{\theta 1} = 0.3C_\theta \quad (79)$$

Figure 6 reports F_C in terms of κ for different values of R and Pr . For $Pr = 0.01$, at the relatively small Reynolds number, the temperature spectrum does not follow the law $\kappa^{-5/3}$, thus C_θ is not defined, whereas at $R = 300$ the diagram shows a region with a local maximum where the variations of F_C are relatively small. This maximum identifies C_θ which results to be about 1.5 ($C_{\theta 1} \simeq 0.45$). For $Pr = 0.1$, the larger scaling interval, implies a wider range where $F_C(\kappa) \simeq \text{const}$, for each Reynolds number, resulting now $C_\theta \simeq 1.8$ ($C_{\theta 1} \simeq 0.54$). When $Pr = O(1)$ (0.7 in the figure), the scaling law κ^{-1} , determines that F_C slightly rises with κ , ranging from 1.4 to 2 ($C_{\theta 1} \simeq 0.42 \div 0.58$), values comparable with those obtained in Mydlarski & Warhaft (1998). For $Pr = 10$, the region width where $\Theta \approx \kappa^{-1}$ increases, thus C_θ is not defined.

The scaling law k^{-1} is in line with the theoretical arguments proposed in Batchelor (1959), where

$$\Theta(\kappa) = C_B\sqrt{\frac{\nu}{\epsilon}}\epsilon_\theta\kappa^{-1}, \quad (80)$$

in the viscous–convective range, where $C_B = O(1)$ is the Batchelor’s constant. The present analysis identifies C_B through the temperature spectra previously calculated. To this end, the following quantity

$$F_B(\kappa) = \Theta(\kappa)\kappa\sqrt{\frac{\epsilon}{\nu}}\epsilon_\theta^{-1} \quad (81)$$

here called Batchelor’s function, is first calculated in function of κ , for several values of Re and Pr . The Batchelor’s constant is estimated as $C_\theta = F_B(\kappa)$

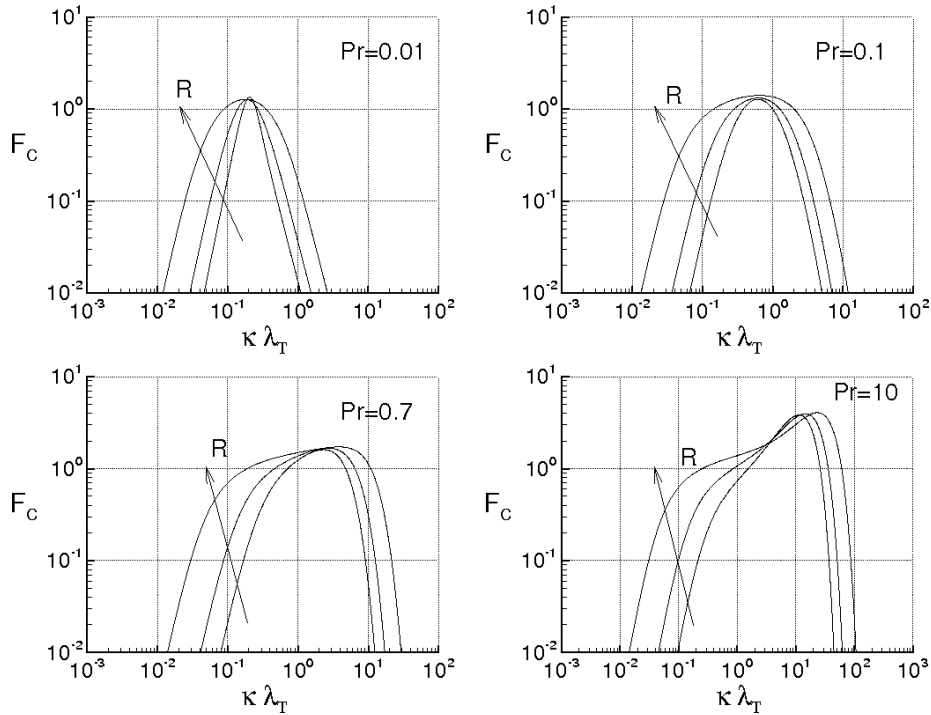


Figure 6: Corrsin function for $R= 50, 100$ and 300 , at different values of Prandtl's numbers.

in the region where $F_B(\kappa) \approx \text{const}$ (or at least exhibits a plateau). The Batchelor's constant C_{B1} can be defined with respect to the one dimensional spectrum (79)

$$\Theta_1(\kappa_1) = C_{B1} \sqrt{\frac{\nu}{\epsilon}} \epsilon_\theta \kappa_1^{-1}, \quad \text{where } C_{B1} = 0.5C_B \quad (82)$$

In Fig. 7, F_B is represented versus κ for different values of Re and Pr . It is apparent that $F_B \approx \text{const}$ when Pr is high enough. For $Pr = 10$, when $R= 50, 100$ and 300 , the values of C_B are about 5, 7 and 8, respectively (that is $C_{B1} \simeq 2.5, 3.5$ and 4) and this occurs for $1 < \kappa < 10$. These values are in quite good agreement with Donzis et al (2010) (and references therein), and are consistent with the experiments of Grant et al (1968) and Oakey (1982) which deal with the temperature spectrum observed in the ocean.

Next, in order to analyse the statistics of the temperature derivative, the PDF of $\partial\vartheta/\partial r$ is calculated with Eqs. (53) and (49), in function of the parameter $\psi = C\sqrt{Pr} R$. This PDF is obtained with sequences of the variables

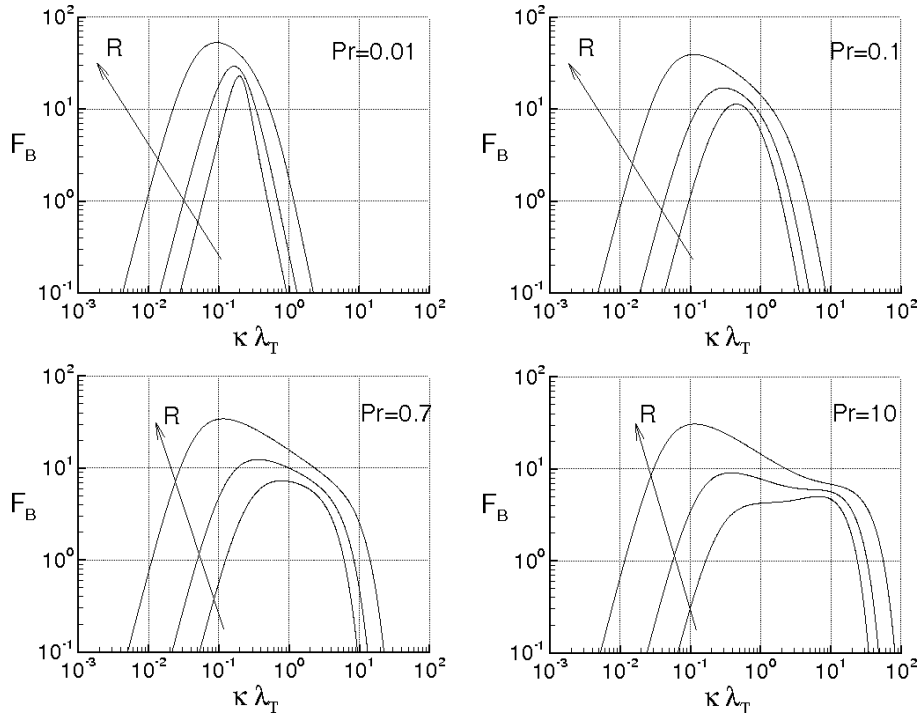


Figure 7: Batchelor's function for $R= 50, 100$ and 300 , at different values of Prandtl's numbers.

ξ , η and ζ , each generated by a gaussian random numbers generator. The distribution function is then calculated through the statistical elaboration of these data and Eq. (49). The corresponding results are shown in Fig. 8, where the PDF is shown in terms of the dimensionless abscissa

$$s = \frac{\partial\vartheta/\partial r}{\sqrt{\langle\partial\vartheta/\partial r^2\rangle}} \quad (83)$$

These distribution functions are normalized, in order that their standard deviations are equal to the unity. These PDFs are even functions of s and their tails rise with ψ in such a way that the intermittency of $\partial\vartheta/\partial r$ increases with ψ , according to Eq. (54). In the figure, the PDFs are calculated for $\psi = 0, 0.25, 0.5, 1., 10., \infty$. For $\psi = 10$ and ∞ , the two curves are about overlapped. More in detail, Fig. 9 shows the PDFs in function of $|s|$ in logarithmic scale. For large Péclet numbers, the PDF varies according to s^{-m} (dashed line) with $m \simeq 3$ in the interval $2 \lesssim s \lesssim 4$, whereas for $s \gtrsim 4$ the exponent m exhibits higher values. This is consistent with

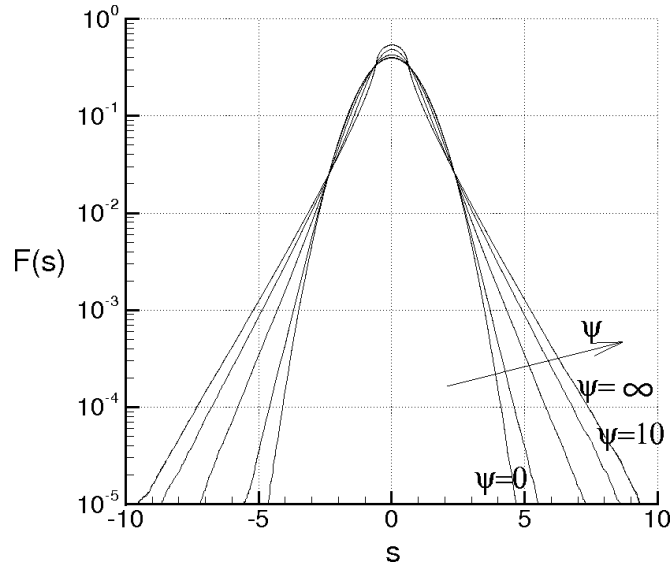


Figure 8: Distribution function of the longitudinal temperature derivatives, at different values of $\psi = C\sqrt{Pr} R$

the results obtained by Fereday & Haynes (2004) which regard the PDF of the scalar concentration. It is worth remarking that the present results deal with the temperature derivative in isotropic turbulence, whereas the data of Fereday & Haynes (2004) concern the intermittency of the scalar concentration. Nevertheless, this comparison can be considered adequate, since, in isotropic turbulence, $\partial\vartheta/\partial r$ exhibits an intermittency which varies with Pe , whereas ϑ remains a gaussian random variable.

To study the intermittency, the flatness H_4 and the hyperflatness H_6 , defined as

$$H_4 = \frac{\langle s^4 \rangle}{\langle s^2 \rangle^2}, \quad H_6 = \frac{\langle s^6 \rangle}{\langle s^2 \rangle^3} \quad (84)$$

are shown in Fig. 10 in function of ψ . For $\psi = 0$, the PDF is gaussian, thus $H_4 = 3$ and $H_6 = 15$. Increasing ψ , the non-linear terms η and ζ determine an increment of H_4 and H_6 , and when $\psi \rightarrow \infty$ $H_4 \rightarrow 9$ and $H_6 \rightarrow 225$. These results are compared with the experiments of Sreenivasan et al (1980). In particular, the value of C identified through the data of Sreenivasan et al (1980) is $C \simeq 0.135$ against the value $C \simeq 0.141$ here calculated.

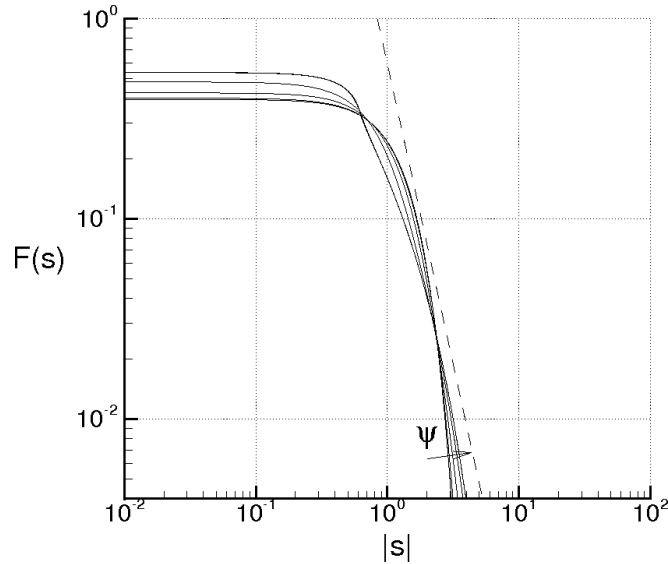


Figure 9: PDF in function of $|s|$

Next, the statistics of the temperature dissipation

$$\varphi = \chi \nabla \vartheta \cdot \nabla \vartheta, \quad (85)$$

is analyzed in function of the Reynolds number. For this purpose, the Kurtosis of φ , $K_4(\varphi)$, is calculated with Eq.(49), taking into account that, due to isotropy, the three components of $\nabla \vartheta \equiv (\vartheta_x, \vartheta_y, \vartheta_z)$ are identically distributed. Furthermore, ϑ_x , ϑ_y and ϑ_z are supposed to be statistically uncorrelated and this allows to analytically express $K_4(\varphi)$ in terms of the dimensionless statistical moments of $\partial \vartheta / \partial r$, according to

$$K_4(\varphi) = \frac{H_8 - 4H_6 + 6H_4 - 3}{3(H_4^2 + 1 - 2H_4)} + 2 \quad (86)$$

where H_4 , H_6 and H_8 are calculated with Eq. (54). Figure 11 shows $K_4(\varphi)$ in function of ψ , and compares the values calculated with the present theory (solid line), with the kurtosis of the scalar energy dissipation obtained by Burton (2008) through the nonlinear large-eddy simulations (symbols). The comparison shows that the data are in qualitatively good agreement. More in detail, for $\psi \rightarrow \infty$, $K_4 = 55$, whereas the results of Burton (2008) give a value of about 60. This difference could be due to the fact that the present analysis considers only the isotropic turbulence which tends to reduce the

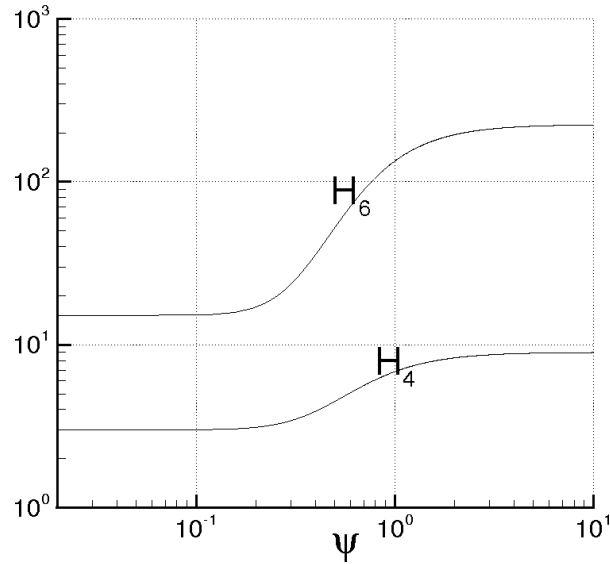


Figure 10: Dimensionless statistical moments, H_4 and H_6 of $\partial\vartheta/\partial r$ in function of ψ .

absolute dimensionless statistical moments of $\partial\vartheta/\partial r$ and of φ , whereas the results of Burton (2008) arise from the nonlinear large-eddy simulations. Next, in our calculation the components of $\nabla\vartheta$ are assumed to be statistically uncorrelated.

9. Conclusions

The finite-scale Lyapunov theory is adopted to study the temperature fluctuations in homogeneous isotropic turbulence. This analysis leads to the closure of the Corrsin equation and provides the statistics of temperature fluctuations. The results, which represent a further application of the analysis presented in de Divitiis (2010) and de Divitiis (2011), are here obtained in the case of self-similar velocity and temperature fluctuations, and can be so summarized:

1. The energy equation, formally written using the referential coordinates and the Lyapunov analysis of the local deformation, allows to factorize the temperature fluctuation and to express it in the Lyapunov exponential form of the local deformation.

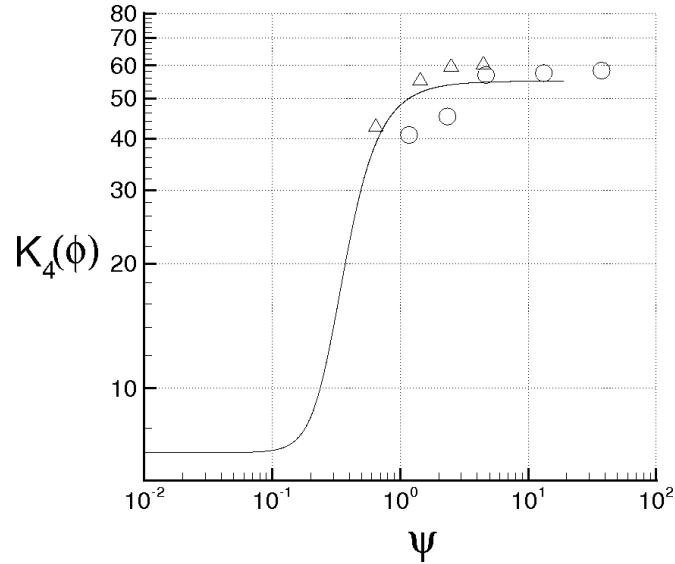


Figure 11: Comparison of the results: Kurtosis of temperature dissipation in function of ψ . The symbols represent the result by Burton (2008).

2. The finite-scale Lyapunov analysis provides an explanation of the physical mechanism of thermal energy cascade and leads to the closure of the Corrsin equation. This is a non-diffusive closure equation which expresses G in terms of f and $\partial f_\theta / \partial r$.
3. The closed Corrsin equation generates temperature spectra with different scaling laws, depending on R and Pr . In particular, for the proper values of R and Pr , these spectra satisfy the Corrsin–Obukhov and Batchelor scaling laws in opportune intervals of the wave-numbers.
4. The Corrsin–Obukhov and Batchelor constants, here identified with the proposed theory, agree with the different source from the literature.
5. The PDF of ϑ_r and the corresponding dimensionless moments, are determined through a canonical decomposition of velocity and temperature in terms of proper random variables which describe the mechanism of energy cascade. This is a non-Gaussian PDF whose intermittency increases with R and Pr , in agreement with experiments and simulations of prior studies.

10. Acknowledgments

This work was partially supported by the Italian Ministry for the Universities and Scientific and Technological Research (MIUR).

11. Appendix

For the sake of convenience, this section reports the main results of the finite scale Lyapunov analysis obtained by de Divitiis (2010) and de Divitiis (2011), which deal with the homogeneous isotropic turbulence.

11.1. Closure of the von Kármán–Howarth equation

In fully developed isotropic homogeneous turbulence, f satisfies the von Kármán–Howarth equation (von Kármán & Howarth (1938))

$$\frac{\partial f}{\partial t} = \frac{K(r)}{u^2} + 2\nu \left(\frac{\partial^2 f}{\partial r^2} + \frac{4}{r} \frac{\partial f}{\partial r} \right) + \frac{10\nu}{\lambda_T^2} f \quad (87)$$

the boundary conditions of which are

$$\begin{aligned} f(0) &= 1, \\ \lim_{r \rightarrow \infty} f(r) &= 0 \end{aligned} \quad (88)$$

where $\lambda_T \equiv \sqrt{-1/f''(0)}$ is the Taylor scale, and u is the standard deviation of u_r , which satisfies the equation of the turbulent kinetic energy

$$\frac{du^2}{dt} = -\frac{10\nu}{\lambda_T^2} u^2 \quad (89)$$

The function $K(r)$, related to the triple velocity correlation, represents the effect of the inertia forces and expresses the mechanism of energy cascade. Thus, the von Kármán–Howarth equation provides the relationship between $\langle (\Delta u_r)^2 \rangle$ and $\langle (\Delta u_r)^3 \rangle$, where Δu_r is the longitudinal velocity difference.

The Lyapunov theory proposed in de Divitiis (2010) leads to the closure of the von Kármán–Howarth equation, and expresses $K(r)$ in terms of f and $\partial f / \partial r$

$$K(r) = u^3 \sqrt{\frac{1-f}{2}} \frac{\partial f}{\partial r} \quad (90)$$

$K(0) = 0$ and this represents the property that K does not modify the fluid kinetic energy (von Kármán & Howarth (1938), Batchelor (1953)).

11.2. Statistics of the longitudinal velocity difference

Here, the results of de Divitiis (2010), dealing with the statistics of Δu_r are recalled. There, Δu_r is represented in terms of centered random variables

$$\frac{\Delta u_r}{\sqrt{\langle (\Delta u_r)^2 \rangle}} = \frac{\xi_u + \psi_u (\chi(\eta_u^2 - 1) - (\zeta_u^2 - 1))}{\sqrt{1 + 2\psi_u^2(1 + \chi^2)}} \quad (91)$$

where ψ_u is a function of r and of the Taylor-scale Reynolds number

$$\psi_u(\mathbf{r}, R) = \sqrt{\frac{R}{15\sqrt{15}}} \hat{\psi}_u(r) \quad (92)$$

$\psi_{u0} = \psi_u(R, 0)$, with $\hat{\psi}_u(0) = 1.075$, and $\chi \neq 1$ gives a nonzero skewness of Δu_r (de Divitiis (2010)). Equation (91) arises from statistical considerations about the Fourier-transformed Navier–Stokes equations and expresses the internal structure of fully developed isotropic turbulence, where ξ_u , η_u and ζ_u are independent centered random variables which exhibit gaussian PDFs $p(\xi_u)$, $p(\eta_u)$ and $p(\zeta_u)$ whose standard deviations are equal to the unity.

11.3. Self-Similarity in homogeneous isotropic turbulence

Now, the results of the self-similarity are briefly summarized. These are based on the idea that far from the initial condition, the combined effects of energy cascade and viscosity act keeping f and $E(\kappa)$, similar in time for large values of wavelengths (von Kármán & Howarth (1938); von Kármán & Lin (1949)). This condition, applied to Eq. (87), leads to the following ordinary differential equation

$$\sqrt{\frac{1-f}{2}} \frac{df}{d\hat{r}} + \frac{2}{R} \left(\frac{d^2 f}{d\hat{r}^2} + \frac{4}{\hat{r}} \frac{df}{d\hat{r}} \right) + \frac{10}{R} f = 0 \quad (93)$$

Into Eq. (93), $f = f(\hat{r})$, where $\hat{r} = r/\lambda_T(t)$, therefore $d^2 f/d\hat{r}^2(0) = -1$. This similarity and the equation of u^2 lead to the expressions of u and λ_T

$$\lambda_T(t) = \lambda_T(0) \sqrt{1 + 10\nu t/\lambda_T^2(0)}, \quad u(t) = \frac{u(0)}{\sqrt{1 + 10\nu t/\lambda_T^2(0)}}. \quad (94)$$

As the solutions $f \in C^2 [0, \infty)$ with $df/d\hat{r}(0) = 0$ tend to zero when $r \rightarrow \infty$, the boundary condition (88) is replaced by the following conditions in the origin

$$f(0) = 1, \quad \frac{df(0)}{d\hat{r}} = 0 \quad (95)$$

Therefore, the boundary problem represented by Eqs. (93) and (88), can be reduced to an initial condition problem written in the Cauchy's normal form

$$\begin{aligned} \frac{df}{d\hat{r}} &= F \\ \frac{dF}{d\hat{r}} &= -5f - \left(\frac{1}{2} \sqrt{\frac{1-f}{2}} R + \frac{4}{\hat{r}} \right) F \end{aligned} \quad (96)$$

the initial condition of which is

$$f(0) = 1, \quad F(0) = 0 \quad (97)$$

References

- ANTONIA R. A., SMALLEY R. J., ZHOU T., ANSELMET F., DANAILA L., Similarity solution of temperature structure functions in decaying homogeneous isotropic turbulence, *Phys. Rev. E*, **69**, 016305, 2004, DOI: 10.1103/PhysRevE.69.016305
- BAEV M. K., CHERNYKH G. G., On Corrsin equation closure, *Journal of Engineering Thermophysics*, **19**, pp. 154–169, no. 3, DOI: 10.1134/S1810232810030069
- BATCHELOR, G. K., Small-scale variation of convected quantities like temperature in turbulent fluid. Part 1. General discussion and the case of small conductivity, *Journal of Fluid Mechanics*, **5**, 1959, pp. 113–133
- BATCHELOR G. K., HOWELLS I. D., TOWNSEND A. A., Small-scale variation of convected quantities like temperature in turbulent fluid. Part 2. The case of large conductivity, *Journal of Fluid Mechanics*, **5**, 1959, pp. 134–139

- BATCHELOR G. K., *The Theory of Homogeneous Turbulence*. Cambridge University Press, Cambridge, 1953.
- BURTON G.C., The nonlinear large-eddy simulation method applied to and passive-scalar mixing, *Phys. Fluids*, **20**,035103, 2008, DOI: <http://dx.doi.org/10.1063/1.2840199>
- CHASNOV, J., CANUTO V. M., ROGALLO R. S., Turbulence spectrum of strongly conductive temperature field in a rapidly stirred fluid. *Phys. Fluids A*, **1**, pp. 1698-1700, 1989, doi:10.1063/1.857535.
- CORRSIN S., The Decay of Isotropic Temperature Fluctuations in an Isotropic Turbulence, *Journal of Aeronautical Science*, **18**, pp. 417-423, no. 12, 1951.
- CORRSIN S., On the Spectrum of Isotropic Temperature Fluctuations in an Isotropic Turbulence, *Journal of Applied Physics*, **22**, pp. 469-473, no. 4, 1951., DOI: 10.1063/1.1699986.
- DE DIVITIIS N., Lyapunov Analysis for Fully developed Homogeneous Isotropic Turbulence, *Theoretical and Computational Fluid Dynamics*, DOI: 10.1007/s00162-010-0211-9.
- DE DIVITIIS N., Self-Similarity in Fully Developed Homogeneous Isotropic Turbulence Using the Lyapunov Analysis, *Theoretical and Computational Fluid Dynamics*, DOI: 10.1007/s00162-010-0213-7.
- DE DIVITIIS N., Refinement of a Previous Hypothesis of the Lyapunov Analysis of Isotropic Turbulence, *Journal of Engineering*, vol. 2013, Article ID 653027, 4 pages, 2013. doi:10.1155/2013/653027.
- DOERING C.R. AND THIFFEAULT JL., Multiscale mixing efficiencies for steady sources, *Phys. Rev. E*, **74**,025301(R), 2006, DOI: <http://dx.doi.org/10.1103/PhysRevE.74.025301>.
- DONZIS D. A., SREENIVASAN K. R., YEUNG P. K., The Batchelor Spectrum for Mixing of Passive Scalars in Isotropic Turbulence, *Flow, Turbulence and Combustion*, **85**, pp. 549-566, no. 3-4, DOI: 10.1007/s10494-010-9271-6

- FEREDAY D. R. AND HAYNES P. H., Scalar decay in two-dimensional chaotic advection and Batchelor-regime turbulence, *Phys. Fluids*, **16**,4359, 2004, DOI: <http://dx.doi.org/10.1063/1.1807431>.
- GEORGE W. K., A theory for the self-preservation of temperature fluctuations in isotropic turbulence. Technical Report 117, Turbulence Research Laboratory, January 1988.
- GEORGE W. K., "Self-preservation of temperature fluctuations in isotropic turbulence," in *Studies in Turbulence*, Springer, Berlin, 1992.
- GIBSON, C. H., SCHWARZ W. H., The Universal Equilibrium Spectra of Turbulent Velocity and Scalar Fields, *Journal of Fluid Mechanics*, **16**, 1963, pp. 365–384
- GRANT, H.L., HUGHES, B.A., VOGEL, W.M., MOILLIET, A., Spectrum of temperature fluctuations in turbulent flow, *Journal of Fluid Mechanics*, **34**, 1968, pp. 423-442
- VON KÁRMÁN, T., HOWARTH, L., On the Statistical Theory of Isotropic Turbulence., *Proc. Roy. Soc. A*, **164**, 14, 192, 1938.
- VON KÁRMÁN, T., LIN, C. C., On the Concept of Similarity in the Theory of Isotropic Turbulence., *Reviews of Modern Physics*, **21**, 3, 516, 1949.
- LEHMANN, E. L., *Elements of Large-sample Theory*. Springer, 1999.
- MADOW, W. G., Limiting Distributions of Quadratic and Bilinear Forms., *The Annals of Mathematical Statistics*, Vol. 11, No. 2, (Jun. 1940), 125–146, 1940.
- MILLS, R. R. JR., KISTLER, A. L., O'BRIEN, V., CORRISIN, S., Turbulence and temperature fluctuations behind a heated grid, NACA-TN-4288, August 1958.
- MYDLARSKI, L., WARHAFT, Z., Passive scalar statistics in high-Péclet-number grid turbulence, *Journal of Fluid Mechanics*, **358**, 1998, pp. 135–175
- OAKEY, N. S., Determination of the rate of dissipation of turbulent energy from simultaneous temperature and velocity shear microstructure measurements, *J. Phys. Oceanogr.*, **12**, 1982, pp. 256-271

- OBUKHOV, A. M., The structure of the temperature field in a turbulent flow. *Dokl. Akad. Nauk.*, CCCP, **39**, 1949, pp. 391.
- OGURA, Y., Temperature Fluctuations in an Isotropic Turbulent Flow, *Journal of Meteorology*, **15**, 1958, pp. 539-546
- SCHEKOCHIHIN A.A., HAYNES P.H., AND COWLEY S.C., Diffusion of passive scalar in a finite-scale random flow, *Phys. Rev. E*, **70**,046304, 2004, DOI: <http://dx.doi.org/10.1103/PhysRevE.70.046304>.
- SREENIVASAN K. R., TAVOULARIS S., HENRY R., CORRSIN S., Temperature fluctuations and scales in grid-generated turbulence., *Journal of Fluid Mechanics*, **100**, 1980, pp. 597–621, doi:10.1017/S0022112080001309
- TRAN C.V., An upper bound for passive scalar diffusion in shear flows, *Phys. Fluids*, **19**,068104, 2007, DOI: <http://dx.doi.org/10.1063/1.2744050>.
- TRAN C.V., Constraints on scalar diffusion anomaly in three-dimensional flows having bounded velocity gradients, *Phys. Fluids*, **20**,077103, 2008, DOI: <http://dx.doi.org/10.1063/1.2957022>.
- TRUESDELL, C., *A First Course in Rational Continuum Mechanics*, Academic, New York, 1977.
- VENTSEL, E. S., *Theorie des probabilites*. Ed. Mir, CCCP, Moskow, 1973.
- WARHAFT Z., LUMLEY J. L., An experimental study of the decay of temperature fluctuations in grid-generated turbulence. *Journal of Fluid Mechanics*, **88**, 1978, pp. 659–684, doi:10.1017/S0022112078002335